

Review of LoRAWAN and the protocol suitability for low bandwidth wireless sensor networks over 5G

Isaack Adidas Kamanga^{1,2} and Johanson Miserigodiasi Lyimo^{1,2}

¹ Dar es Salaam Institute of Technology (DIT), Dar es Salaam, Tanzania.

² Electronic and telecommunications engineering department, Tanzania.

International Journal of Science and Research Archive, 2022, 07(02), 291–305

Publication history: Received on 11 July 2022; revised on 25 November 2022; accepted on 27 November 2022

Article DOI: <https://doi.org/10.30574/ijrsra.2022.7.2.0273>

Abstract

LoRaWAN is currently the best among the LPWANs protocols when it comes to IoT or machine-to-machine (M2M) communication such as in the deployment of wireless sensor networks. LoRaWAN is an RF technology operating in ISM bands. Its strength comes from the capability of Long-range communication between remote sensors and the gateways, deep indoor penetration, and public and private network deployment. All these traits are possible because of the LoRa network modulation technique. This paper provides an overview of the LoRaWAN protocol and the 5G cellular network. Also, the paper gives the benefits of using LoRaWAN over the other technologies for the deployment of the IoT module communication links.

Keywords: LoRa; LoRaWAN; LPWAN; Chirp Spread Spectrum; LoRaWAN end device

1. Introduction

LoRa stands for Long-range Radio [1], a modulation approach based on the chirp spread spectrum (CSS) technique [2]. Chirp spread spectrum (CSS) is a spread spectrum technology used in telecommunications that encrypts data using wideband linear frequency modulated chirp pulses [1-3]. A chirp is a signal that oscillates between increasing and decreasing frequencies [4], [5]. LoRaWAN is a Wide Area Network (WAN) radio communication protocol based on the LoRa modulation technique. LoRaWAN is one of the most promising communication standards for linking IoT devices [5]. According to [6], it is a leading LPWAN. Low Power Wide Area Network (LPWAN). It is intended to interconnect battery-powered devices over a long range. therefore, LoRaWAN is the media access control (MAC) layer protocol that manages communication between LPWAN devices and gateways. LoRaWAN is an open standard meaning that it is free for anyone to use [7]. LoRaWAN is being supported and promoted by the LoRa Alliance [8], [9].

The members are the various IoT device makers and service providers of technology solutions and networks [10]. Compared to conventional mobile networks, LoRaWAN functions more affordably and with less power consumption. Additionally, it can accommodate more linked devices across a bigger region. LoRaWAN as an example of LPWAN supports uplink rates of up to 200 Kbps and packet sizes ranging from 10 to 1,000 bytes [11]. LoRaWAN focuses on important IoT (internet of things) requirements such as geolocation services, mobility, and secure bi-directional communication. LoRaWAN standard enables the deployment of IoT applications by offering easy interoperability between smart devices without the need for complicated local installations.

* Corresponding author: Isaack Adidas Kamanga, Assistant lecturer, Electronics and Telecommunications Engineering department (ETE), Dar es Salaam Institute of Technology (DIT), Dar es Salaam, Tanzania.

2. The network architecture

LoRaWAN links IoT devices to the network server and manages the dialogue between these devices and the gateways in the network (see Figure 1). In contrast to LoRaWAN, which is an open protocol that enables IoT devices to use LoRa for communication, LoRa is a modulation method for a particular wireless spectrum. The basic network architecture of LoRaWAN is depicted in Figure 1, it consists of the end communication devices, LoRaWAN gateways (often called concentrators), and Network servers (the core network). The internet is not a LoRaWAN, serves as the link between various LoRa gateways and the LoRa network servers.

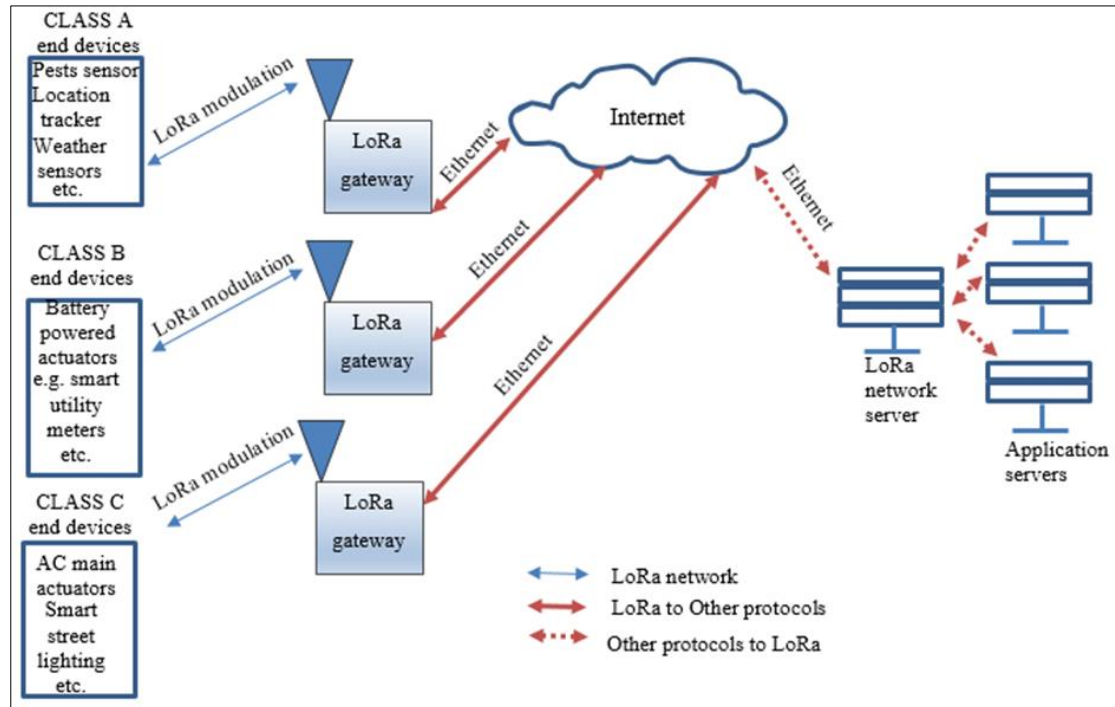


Figure 1 LoRaWAN network architecture

2.1. Network components

The LoRaWAN architecture is composed of the following components.

2.1.1. End devices

LoRaWAN end device or node can either be a sensor or an actuator wirelessly connected to the gateways using LoRa modulated signal. The end devices can be remote sensors, vending machines, pet trackers, car trackers, or any other IoT device. Figure 2 shows examples of end devices and the LoRa gateway.

2.1.2. LoRa gateways

LoRa gateways are the network nodes linking the end devices (by a radio channel) and the network server (the core network). The link between the LoRa gateway and a network server is normally an IP based and can be extended by any layer 2 protocol such as Ethernet, MPLS, Point-to-Point Protocol (PPP), High-level Data Link Control (HDLC), and ATM.

2.2. Network server and application servers

Humans are able to access information from the end devices through the applications running in application servers (such as personal computers). These application servers are connected to the LoRa network server via an IP connection. Figure 2 shows how this component is linked.

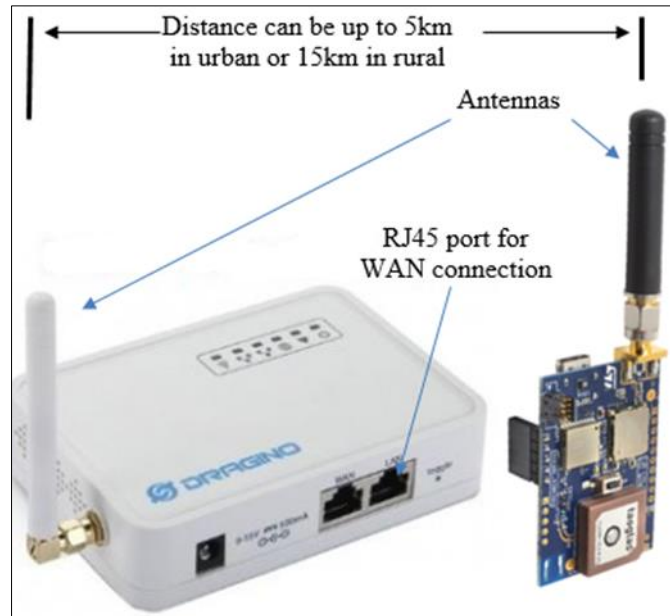


Figure 2 LoRa end device and LoRa gateway

There are two types of LoRa messages exchanged between end devices and LoRa servers, the uplink and downlink messages [12], [13]. Uplink messages are sent by end devices to the network server through one or many concentrators while the downlink messages are sent by the network server to the end device through a single gateway.

2.3. Choosing LoRaWAN end-devices

There are three classes of LoRaWAN end devices in the market based on the MAC layer [14]. There are class A, class B, and class C LoRa end devices [15]. All end devices must have class “A” specifications, class “B” and “C” have class “A” specifications plus some extensions [16], [17]. All LoRa network end devices support half-duplex communication. Class A is the lowest power end-device [18]. In class A communication, the end device can send uplink data at any time. After uplink transmission, an end device opens two short downlink windows, even if a network server did not respond during this time, the next downlink transmission is scheduled after the next uplink transmission. Class A frame has 2 parts, the uplink, and downlink, the uplink has 1 slot while the downlink has 2 slots [19].

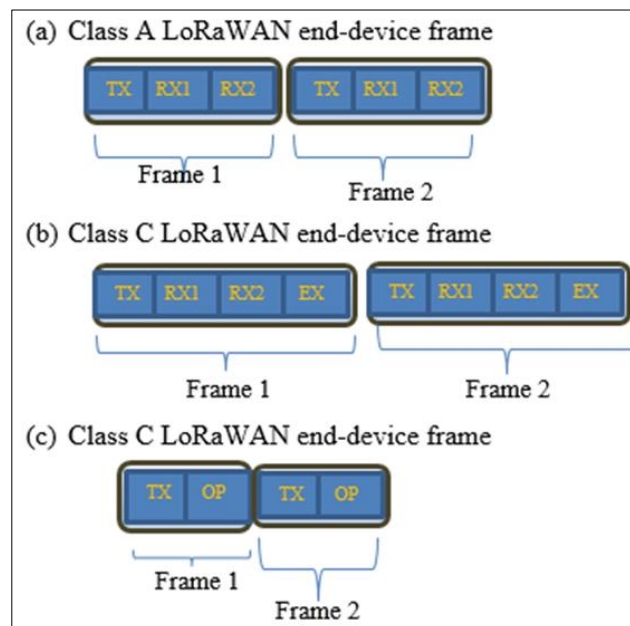


Figure 3 LoRaWAN end device classes

The scheduling of the uplink is done only if needed by the device itself based on a random approach similar to the ALOHA standard. Class “B” end-devices utilize an extra window (EX in Figure 3 (b)) to receive data during the downlink period in addition to the 2-time slots of class A [20]. Class B devices tend to have lower latency compared to class A because they are always in active mode as long as the battery has a charge [21], [22]. According to [1] and [7], class C LoRaWAN end devices always listen to the gateway, and the receive (downlink) is always active (time slot OP in Figure 3 (c)) except during the transmit time (uplink).

In addition to that, class C has a lower latency compared to B devices but has high power consumption compared to both class A and B devices. Class C devices are used when extremely low power consumption is not an issue and latency needs to be eliminated. Figure 3 shows the frame structures of these three classes. In both classes, the uplink window must close during the downlink window, they only operate in half duplex mode. Class A and B devices may switch to class C in a short period of time to update their firmware by a method called Firmware Update Over-The-Air (FUOTA).

The characteristics and areas of application of different LoRa network end devices are summarised in Table 1. The table gives suggestions of the circumstances that may lead to selecting a particular class of LoRa network end-device.

Table 1 Characteristics of each class of LoRa network end-devices and area of application

S/N	Attribute	Class A	Class B	Class C
1	Call initiation	End-device can initiate a call anytime Most of the time they stay in sleep mode	A Server can initiate a call at a fixed interval They are in active mode in the predefined interval for downlink	A Server can initiate a call at any time They are in active mode always
2	Source of power	Battery powered	Battery powered	Mains powered
3	Power consumption	Highly power efficiency Long battery life	Higher power consumption Short battery life	Highest power consumption
4	Latency	There is a delay between the end of the transmission and the beginning of the receive	Low latency between the end of the uplink and the beginning of the downlink window	No latency between the end of the uplink and the beginning of the downlink window
5	Area of application	Remote sensing Crop-pest traps Tracking a location Object/animal tracking Fire detection Environmental monitoring Water leakage detection Earthquake early detection	Electricity utility meters Water utility meters Reporting temperature	Utility meters with cut-off valves/circuit breakers for water and electricity respectively Smart CCTV cameras Streetlights controlling Traffic light

3. Why opt LoRaWAN for IoT over 5G

When compared to other wireless data transmission technologies such as cellular networks, Wi-Fi, Bluetooth, or ZigBee, LoRa is a modulation that offers a noticeably higher communication range with small bandwidths. A communication LoRaWAN protocol uses the LoRa modulation technique to send tiny data such as those from remote sensors across great distances. LoRa networks employ a LoRa modulation technique that facilitates long-distance reliable communication when the data rates are small [7], [11]. According to [1] and [3-6], in urban areas, the LoRa network can

push data between the end device and gateway between 0-5 km while in sparsely populated areas this distance can increase to 15 km. Sending data over LoRa networks consumes less power, and the consumption is extremely low when class A end devices are used [1].

LoRaWAN operates in the ISM band using LoRa modulation, LoRa modulation enables deep penetration of the signal in the walls and in the walls [20]. This allows for example the linking of sensors in the building basements, parking sensors underground, and utility meters.

Moreover, LoRaWAN has flexibility in the deployment. LoRa network can either be deployed as a private network or as a public network [6-8], [20]. In private deployment, all network components are privately owned whilst in public deployment, the WAN connecting the network servers and application server LAN, and gateway-end device LAN belongs to a second-part network operator such as Vodacom, Tigo, and Zantel. Firmware Update Over-The-Air (FUOTA) simplifies the updating of the end devices' LoRa network stack. GPS chips are not required in LoRaWAN nodes and end devices because geolocation is performed using a low-cost Semtech's LoRa Cloud geolocation services [6].

Furthermore, security is another strength of LoRaWAN over the like networks. Two layers of security are provided by LoRaWAN using 128-bit cryptographic keys and algorithms [1-3], [18], [20]. MAC commands are encrypted as part of the first security layer, which is applied between the end device and the network server. The implementation of the second layer of security ensures end-to-end encryption of the application payload between the end device and the application server.

In applications requiring broadband, 5G is useful to provide a high-speed connection between LoRa gateways and the network servers. In application areas such as street lights, agriculture, oil and gas, utility meters, etc. the bandwidth requirement is minimum therefore, the LoRa network fits well compared to 5G due to its characteristics discussed in this section.

LoRa network message capacity is incredible, it can support millions of messages. However, the number of messages in a given deployment shall depend upon the number of signal concentrators installed in that deployment [8], [21].

Up to a few hundred thousand messages can be supported by a single eight-channel concentrator per day [17]. The implementation cost is decreased since a small number of signal concentrators can support thousands of end devices handling millions of LoRa messages [17]. Furthermore, because there isn't a lot of gear to operate and maintain, operational costs are kept to a minimum.

4. LoRa protocol stack

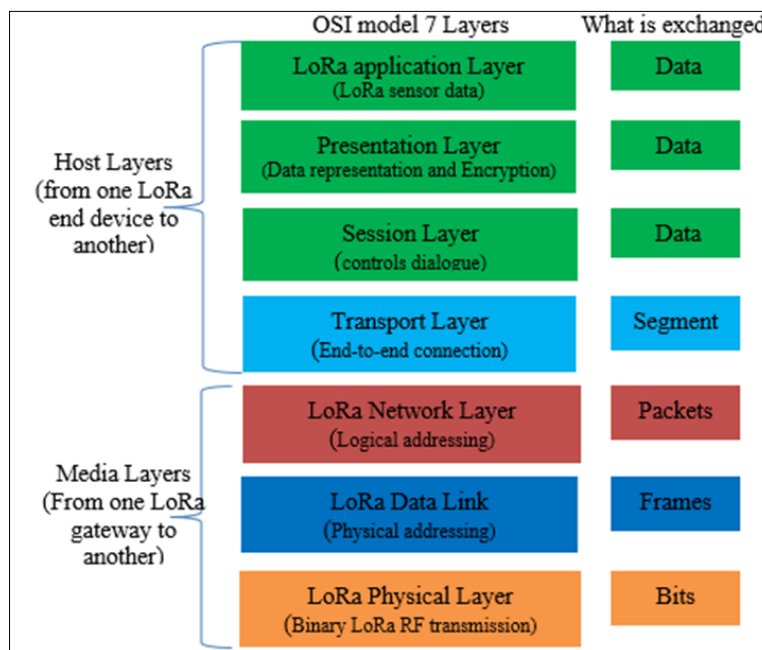


Figure 4 LoRa network protocol stack in OSI model

LoRa standard operates in media layers of the OSI reference model which are the Physical layer, Data link layer, and Network layer [1], [6], [7]. Figure 4 shows where LoRa network standard fits in OSI model.

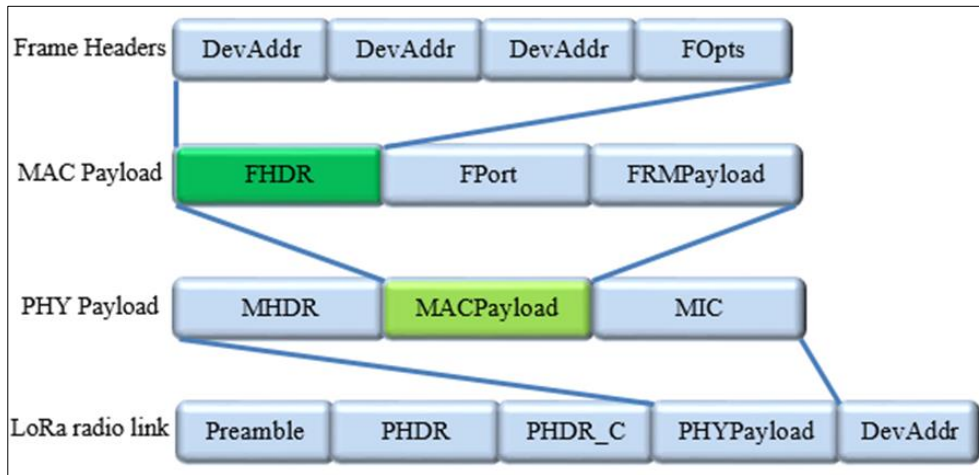


Figure 5 LoRa message formats at different layers

The MAC layer is responsible for the construction of the MAC messages used in the establishment of the dialogue between the end device and the application server. Table 1 shows the LoRa message flags and their descriptions. Furthermore, the LoRaWAN layer deals with logical addressing and transmission of the data packets from the end devices to the application server.

Table 1 LoRa message fields and their corresponding descriptions

S/N	LORA MESSAGE FIELD	FIELD DESCRIPTION
1	MHDR	MAC Header, Single octet long
2	MAC Payload	Data from upper layer
3	MIC	Message Integrity Code, 4 octet long
4	FHDR	Frame Header
5	FPort	Optional port field
6	FRMPayload	Optional Frame Payload field
7	Devaddr	Device address
8	FCtrl	Frame Control Octet
9	FCnt	Frame Counter, 2 octets long
10	FOpts	Frame Options used to transport MAC commands, 15 octets long

5. Aspects giving LoRaWAN credits over 5G network

There are certain traits that give LoRaWAN network protocol added advantages over the use of other network standards. However, the integration of LoRaWAN with 5G is essential to provide quick backbone links.

5.1. Chirp Spread Spectrum (CSS) modulation technique

LoRaWAN uses a chirp spread spectrum modulation technique to offer more transmission bandwidth to the data. To achieve this, the data is spread over the bandwidth to take advantage of the spreading gain. In CSS, signal is multiplied by a chirp signal to achieve energy spreading in frequency [10], [11]. The chirp carrier can be linear or non-linear, it can be mathematically modeled by Equation 1.

LoRa offers a trade-off between sensitivity and data rate, while operating in a fixed-bandwidth channel of either 125 KHz or 500 KHz (for uplink channels), and 500 KHz (for downlink channels). Additionally, LoRa uses orthogonal spreading factors. This allows the network to preserve the battery life of connected end nodes by making adaptive optimizations of an individual end node’s power levels and data rates. For example, an end device located close to a gateway should transmit data at a low spreading factor, since very little link budget is needed. However, an end device located several miles from a gateway will need to transmit with a much higher spreading factor. This higher spreading factor provides increased processing gain, and higher reception sensitivity, although the data rate will, necessarily, be lower.

5.1.1. LoRa Physical Layer

The use of CSS in the LoRa wide area network standard is a recent and successful example of employment of chirp signals to wireless communications. Notably, LoRa’s PHY employs CSS in conjunction with a variant of FSK modulation as described above [14], [17]. It is important to note that in this case, the discrete chirp rate is set to the unity, and the receiver employs non-coherent detection. Moreover, LoRa PHY defines the SF as the amount of bits that one symbol carries, which ranges from 6 to 12 bits. In short, Fig. 1 presents the discrete-time baseband LoRa PHY transceiver block diagram. The bit-word b contains SF bits that are mapped into one symbol k , which feeds the CSS modulator. The despreading operation at the receiver side is accomplished by multiplying the received signal with a down-chirp, which is obtained by conjugating the up-chirp signal. At the receiver side, the estimated data symbol is obtained by selecting the frequency index with maximum value. The spreading gain, also known as processing gain, is defined by the ratio between the bandwidths of the spreading signal and of the information signal, and for LoRa’s PHY it can be defined in dB as

$$G = 10 \log_{10} \left(\frac{N}{FS} \right) \tag{1}$$

and as $N = 2^{FS}$, the SF also directly relates to the performance improvement observed with a spread spectrum system when compared to a non-spread system. This is analogous to the performance enhancement achieved via coding schemes. Larger SFs correspond to lower code rates, and the improvement obtained comes at the cost of reduced data rate. Therefore, the SF is used as adaptive modulation parameter depending on the signal-to-noise ratio (SNR), and consequently larger SFs allow longer coverage ranges with reduced data rates. A key aspect of LoRa PHY is the fact that channel estimation and equalization are not necessary, since it employs the non-coherent detection receiver. However, employing coherent detection will improve the EE performance of LoRa, since the imaginary noise component is not taken in the estimation of the received data symbol. Furthermore, under harsher multipath, i.e., frequency selective, channel conditions the original LoRa modulation symbol performance can degrade significantly, as also observed in [18]

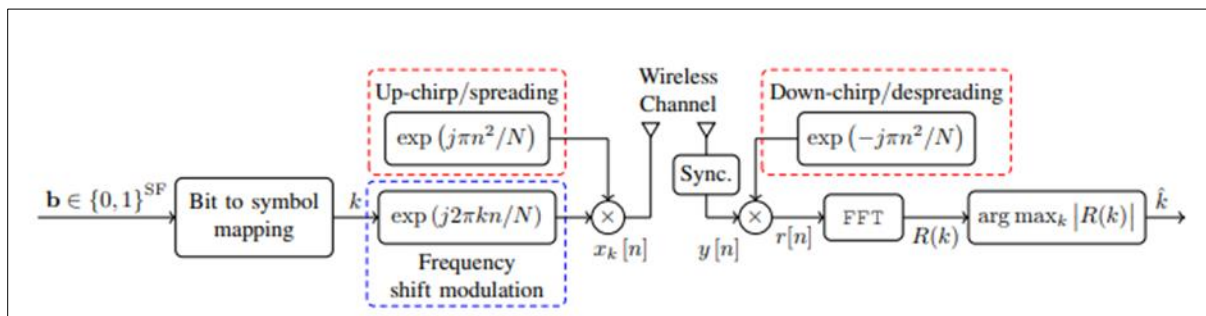


Figure 6 LoRa PHY transceiver block diagram

5.1.2. In-phase and Quadrature CSS

In Quadrature CSS (IQCSS), information is encoded in both in-phase (real) and quadrature (imaginary) components of the transmit signal [13]. By making use of the orthogonality between the sine and cosine waves it is possible to transmit simultaneously two data symbols. Its transmit signal is given by equation (2).

$$X_{k_i}, K_g[n] = \sqrt{\frac{E_s}{2N}} g_{k_i, k_g}[n] c[n] \tag{2}$$

Where by

$$X_{k_i, k_g}[n] = \exp(j \frac{2\pi}{N} k_i n) + j \exp(j \frac{2\pi}{N} k_g n)$$

where k_i and k_g are independent identically (uniform) distributed data symbols drawn from K , and each carries SF bits. Thus, the total amount of transmitted bits is doubled when compared to the LoRa PHY specification. Fig. 3 illustrates the discrete-time baseband IQCSS transceiver block diagram. Note that the additional operations performed at the receiver side do not require modifications on the LoRa's transmit signal structure, since IQCSS makes use of the already available synchronization preamble for channel estimation and subsequent coherent detection. Fig. 2 illustrates one LoRa PHY packet, where there are 14 modulated chirps in the data payload, 10 up-chirps are available for synchronization, followed by 2 down-chirps that indicate the beginning of the data symbols, and are named start frame delimiter (SFD) [14]. The received signal after equalization and despreading is given by equation (3)

$$\bar{r}[n] = g_{k_i, k_g}[n] + w[n] \tag{3}$$

It is important to point out that IQCSS requires coherent detection to work. Therefore, for making further use of the information carried with the synchronization preamble, we propose to use the least squares (LS) approach for estimating the channel gain using the already available preamble structure for synchronization.

Assuming that the channel presents flat-fading within its bandwidth, the received preamble can be represented by equation (4)

$$Y_p[n] = h x_p[n] + w[n] \tag{4}$$

where $x_p[n]$ represents the 10 up-chirps transmitted at the beginning of the LoRa PHY packet, $w[n]$ is AWGN with zero mean and σ^2 variance, and h is the complex-valued channel gain. Consequently, the LS error criterion, which is the squared difference between the received data and the signal model [5], is given by equation (5)

$$J(h) = \sum_{n=0}^{N_p-1} (y_p[n] - h x_p[n])^2 \tag{5}$$

where $N_p = 10^N$ is the preamble length in samples. Differentiating equation (5) w.r.t. h , and setting the result to zero yields to equation (6)

$$h = \frac{X_p^H Y_p}{X_p^H X_p} \tag{6}$$

where x_p and y_p are $N_p \times 1$ vectors whose entries are the samples from $x_p[n]$ and $y_p[n]$, respectively, and \hat{h} is the estimated channel gain. For the case of frequency selective channels, the received preamble is given by equation (7)

$$Y_p[n] = h[n] * X_p[n] + w[n] \tag{7}$$

where $h[n]$ represents the discrete-time channel impulse response with L taps. Under the assumption of a CP appended to the beginning of each chirp, the linear convolution in (7) becomes circular. Thus, after CP removal, the i -th received chirp from the preamble can be written in matrix form as equation (8)

$$Y_p^{(i)} = H X_p^{(i)} + w \tag{8}$$

where $x_p^{(i)} \in \mathbb{C}^{N \times 1}$ contains the samples from the i -th up chirp in the synchronization preamble. Moreover, considering the commutative property of the convolution, equation (8) can be reformulated as equation (9).

$$Y_p^{(i)} = C h + w \tag{9}$$

$$C \in \mathbb{C}^{N \times N}$$

where $C \in \mathbb{C}^{N \times N}$ is a circulant matrix obtained from one raw up-chirp, and $h \in \mathbb{C}^{N \times 1}$ contains the channel impulse response in its first L entries. Therefore, the LS approach can be extended to frequency selective channels. However, as mentioned, a CP needs to be added to the preamble.

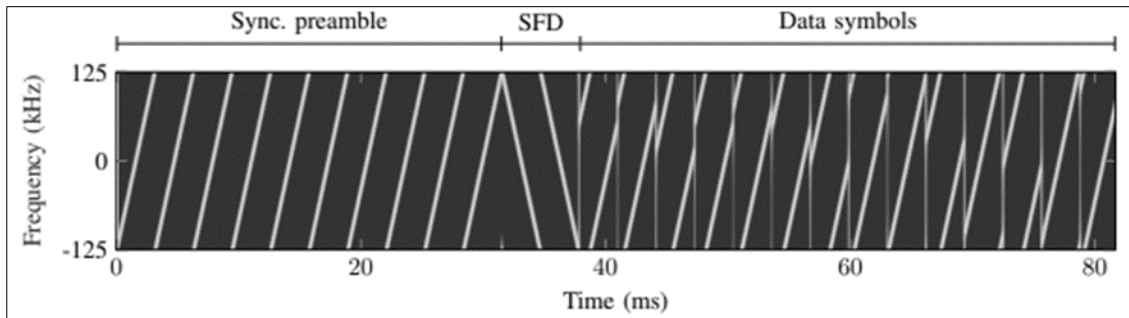


Figure 7 Spectrogram of the LoRa PHY packet structure

5.2. Implementation

LoRaWAN can be integrated with 5G to complement each other. The high-bandwidth, low-latency capabilities of 5G remain crucial for data-intensive ecosystems that require real-time, robust communication. Integration is also possible at the RAN level by merging LoRaWAN with the eNodeB. So the eNodeB would be able to receive LoRa packets as well as has to be capable of handling 3GPP connections. This approach would ease the deployment of future networks if the eNodeB would support multiple LPWAN technologies. Currently, the 5G infrastructure is arranged to be compatible with cloud platforms by virtualizing the network components. To integrate LoRaWAN with the 5G as a part of the core network, LoRa network server could be installed in the cloud along with the core network components.

The OpenStack cloud platform could be utilized to implement LoRa components as a virtual instance. The OpenStack cloud platform supports dashboard to generate virtual instance on top of Linux operating system installed in physical machine. Figure 8 shows the possibility of integrating LoRaWAN and 5G. It is possible for the cellular network to be a customized one with mobile base stations carried by UAVs [22].

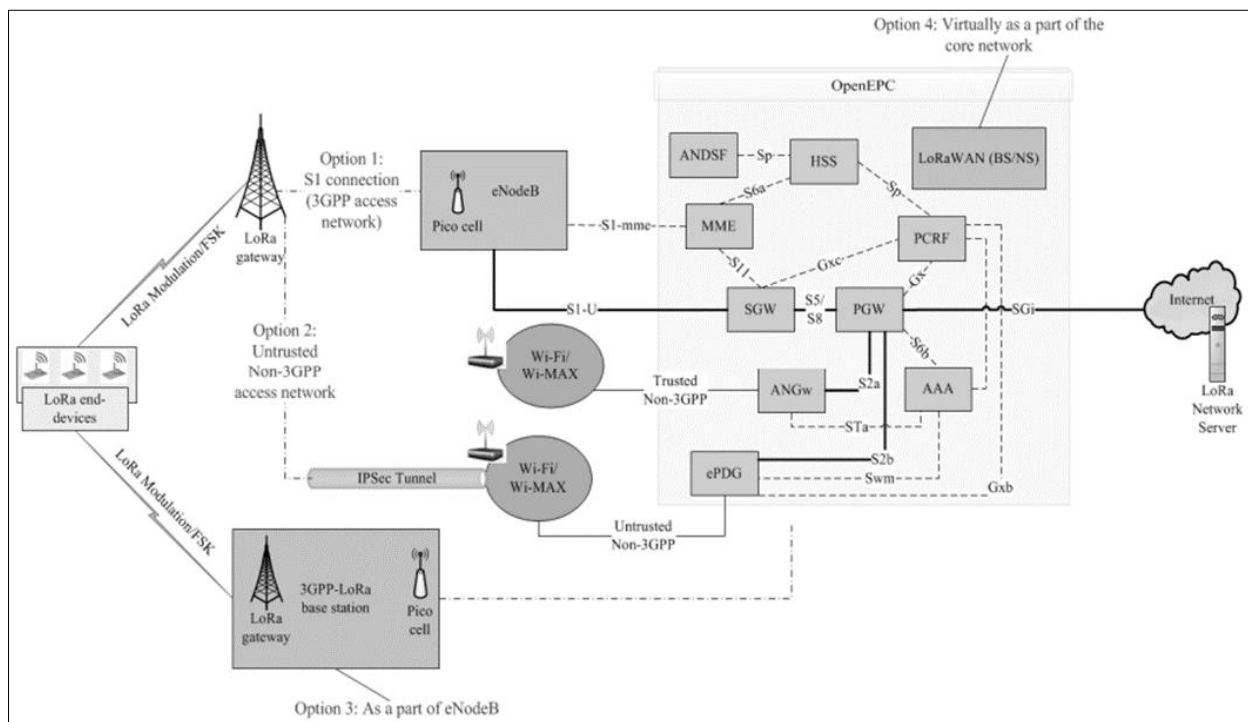


Figure 8 Possibilities of Integration LoRaWAN with the 5GTN

Table shows the comparison of different alternatives of integrating LoRaWAN and 5G cellular network.

Table 2 Different LoRaWAN and cellular networks integration methods and their comparisons

Features	Integration method			
	3GPP access	non-3GPP access	eNodeB integration	virtual in core
communication interface and traffic effects	S1 connection: LPWAN packets added to LTE traffic	WiFi/Wi-MAX: LPWAN packets added to WiFi/Wi-MAX traffic	3GPP backbone: LPWAN packets added to users' traffic	external: LPWAN traffic does not affect core network
security mechanisms ¹	S1 connection	IPSec	S1 connection	Implementation specific
resource management instance	PCRF	ePDG based on PCRF	PCRF	Implementation specific
Hardware & software requirements	gateway must support: LTE connectivity and have an IP stack	gateway must support: WiFi/Wi-MAX connectivity, IP stack, IPSec, 'strongswan'	integration of LoRa gateway with eNodeB is required	OpenStack cloud platform on top of hypervisor
support in today's commercial products	already available	not available	not available	not available
Implementation complexity ²	medium	high	very high	high
Deployment complexity ³	medium	medium	low	high
Scalability	good	good	good	poor
Quality of service	medium	medium	good	Implementation specific

5.3. Simulation and results discussion

The system is evaluated using custom based simulation following [10]. This evaluation focuses on the overall network performance instead of per-node performance. The most economical scenario where m nodes are served by one gateway is observed, presumably to give more insight for early adopter of LoRaWAN technology which is usually not backed up by large amount of funding. The gateway is capable of decoding 8 concurrent orthogonal signals.

In the simulation, the nodes are configured with 5-tuples of settings which specifies the transmission power, carrier frequency, spreading factor, bandwidth, and coding rate. Each node has an average data arrival rate of 10 minutes and a uniform data size of 20 bytes, which is always being transmitted using preamble which consists of 8 symbols. The evaluation is conducted for 2 months.

5.3.1. Assumption and simulation parameters

The performance of the network is measured in term of throughput S and total power consumption P . The throughput S denotes the ratio between number of successfully decoded packet and the total number of transmitted packet. This metric is importance since in the effective LoRaWAN environment all transmitted packet should be received by the backend system. The total power consumption P denotes the number of energy, in Joule (J), spend by the RF module in all transmitting nodes during evaluation. The performance of the network is measured in term of packet delivery ratio (PDR), average energy consumption for each successful transmission E , and average wasted amount of energy per nodes W . The packet delivery ratio denotes the ratio between number of successfully decoded packet and the total number of transmitted packet in the system. This metric is importance since in the effective LoRaWAN environment all transmitted packet should be received by the backend system. Only uplink packet is considered which is consistent with most of the simplified sensor networks in IoT application.

The average energy consumption for each successful transmission E denotes the number of energy, in Joule (J), spend by the RF module in all transmitting nodes during evaluation normalized by number of nodes in the network. With this metric, one can immediately picture the energy cost per data transmission, which can be useful for application designer to decide the frequency of data transmission of the nodes.

The average wasted energy consumption per nodes W denotes the number of energy, in Joule (J), spend by the RF module in each node to transmit the collided packets. It is calculated by multiplying the amount of energy for transmitting one packet and the number of collided packets. With this metric, one can picture how much the energy is wasted and can be useful for application designer to estimate the battery longevity of nodes in respect to the timeliness of its uplink data transmission.

Table 3 shows the simulation parameters used.

5.3.2. Baseline Case

For the sake of comparison with other cases, a baseline case is introduced herein. The baseline case is when all nodes are configured with LoRa common configuration consisting of transmission power of 14 dBm, carrier frequency of 915 MHz, spreading factor of 12, a bandwidth of 125 kHz, and a coding rate of 4/5. Except for the carrier frequency, this setting is similar to the baseline used in [10] and [13]. This baseline case is denoted as “default” in subsequent result figures.

The baseline case and the other cases will be compared under two radio models: the basic model which does not consider the capture effect and the one which considers the capture effect which is more consistent with the LoRa modem. Without capture effect, any two or more transmissions conducted at the same time using the same carrier frequency, spreading factor, and bandwidth will collide and none of them will be successfully decoded. However, with the capture effect, there can be at most one transmission can be recovered from the collision when the difference in timing and strength of the transmitted signals received by the gateway is sufficient.

6. Results and Discussions

Combinations of node configuration play important role in deciding the performance, especially in term of the three metrics used in this paper.

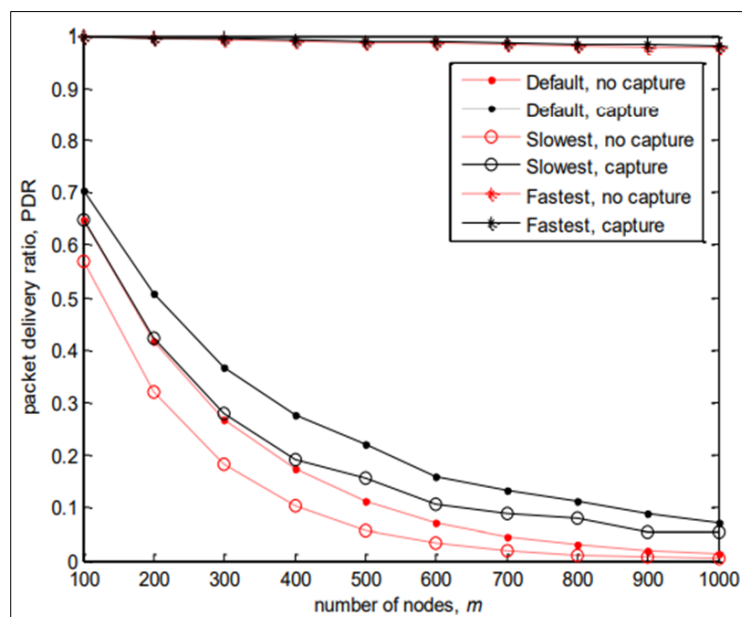


Figure 9 PDR of simulation 1

6.1. Simulation 1

In this experiment, we compare the configuration which favors robustness and the one which favors higher uplink data rate. Notice that these two configurations are the extreme opposite as the most robust configuration has the lowest data

rate and the highest data rate has the worst signal quality. The slowest configuration uses spreading factor of 12, bandwidth of 125 kHz, and coding rate of 4/8. The fastest configuration uses spreading factor of 6, bandwidth of 500 kHz, and coding rate of 4/5. Both of them use transmission power and carrier frequency similar to the one used by the baseline case. The result of PDR from Experiment 1 is shown in Figure 3 along with the default case. Each case is evaluated with and without capture effect. Overall, the cases with capture effect obtain higher PDR compared to the respective cases without capture effect. This is because with capture effect there may be one transmission which can be recovered from each collision. The difference between the fastest case with and without capture effect is not noticeable as both of them are almost visually overlap.

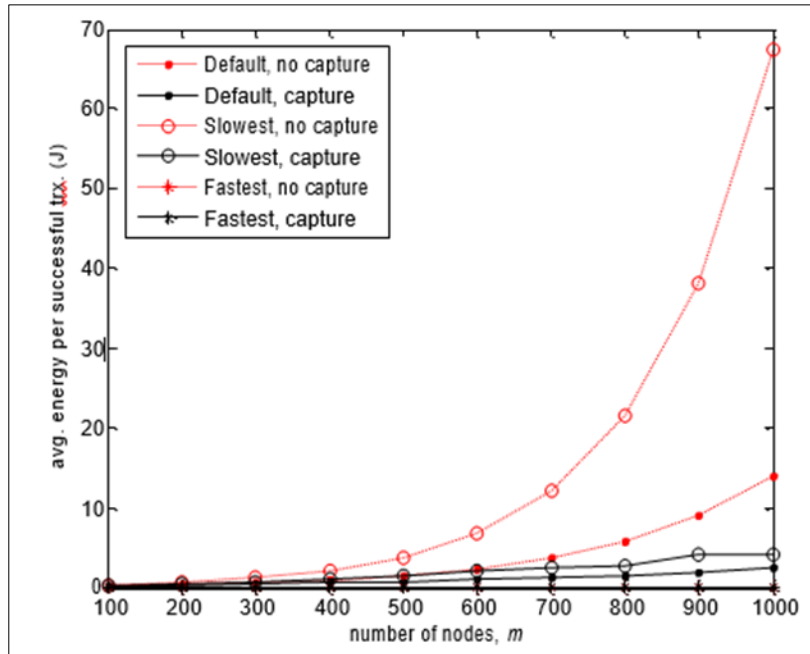


Figure 10 Average Energy Consumption for each Successful Transmission in Experiment 1

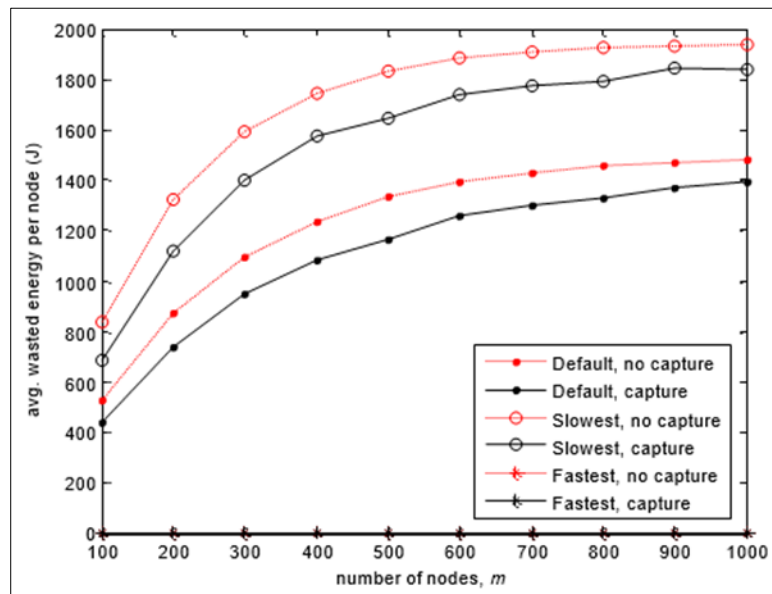


Figure 11 Average Amount of Energy Wasted in Collided Transmissions for each Node in experiment 1

As the name suggests, the slowest configuration delivers lower PDR among the three depicted cases. However, it is closer to the baseline case. Meanwhile, the fastest case delivers the highest PDR out of the three depicted cases. This is because when every transmission signal is received perfectly by the received end, the fastest configuration has shortest airtime or transmission duration. This is important as LoRa has similar access mechanism to pure ALOHA. The longer

transmission duration, the more collision can happen. With shorter transmission duration, other newly-arrived transmission has less chance to overlap with the existing transmission. Hence, with the fastest configuration, more transmission can be successfully received by the gateway which translates to higher PDR.

The result of average energy consumption for each successful transmission E from experiment 1 is depicted in Figure 4 along with the default case. Each case is evaluated with and without capture effect. Notice that E is expected to grow along with number of collision. Since collision rate is the opposite of PDR by the definition, the case which has higher PDR consequently obtains lower E . One thing to be noticed in this figure is that E grows exponentially and a small difference in low PDR translates into significant difference of E . For example, this happens at $m=1000$ between the “Default, no capture” and “Slowest, no capture” cases. In these particular situations, total energy consumption of the default case is somewhere around 1.9 MJ while the slowest case is around 1.5 MJ. Although seemingly both of them have almost similar PDR, the actual number of successful transmission in the default case and slowest case are around 107×10^3 and 28×10^3 , respectively. Thus, their difference in E is large.

The result of average wasted energy consumption per nodes W from experiment 1 is depicted in Figure 5 along with the default case. Each case is evaluated with and without capture effect. From this figure, one can observe that the case with higher PDR yields less wasted energy since there is less number of collided transmissions. The fastest case has the minimum W of 8 mJ and the maximum W of 0.16 J which are depicted as almost 0 in this figure. Meanwhile, the default and the slowest cases obtain significantly higher W , compared to the fastest case, which plots like logarithmic function. With these conditions, the nodes are less effective in using their battery power as it will be consumed a lot by collision.

6.2. Experiment 2: Performance on AWGN channel

For comparing the performance of the proposed schemes against the LoRa PHY, we resort to numerical simulations for estimating the symbol bit error ratio (SER/BER) under three different wireless channel models, namely AWGN, time-variant (TV) non-frequency-selective (Rayleigh) channel, and time-variant frequency-selective (TVFS). For the latter, the channel model chosen is the typical case for urban area with 12 taps [20]. This has been chosen due to the similar operating frequency and bandwidth of LoRa and Global System for Mobile Communications (GSM) in Europe. Moreover, based on the symbol error ratio, the maximum achievable throughput is also presented for supporting the claims of increased spectral efficiency. Table 3 shows the simulation parameters.

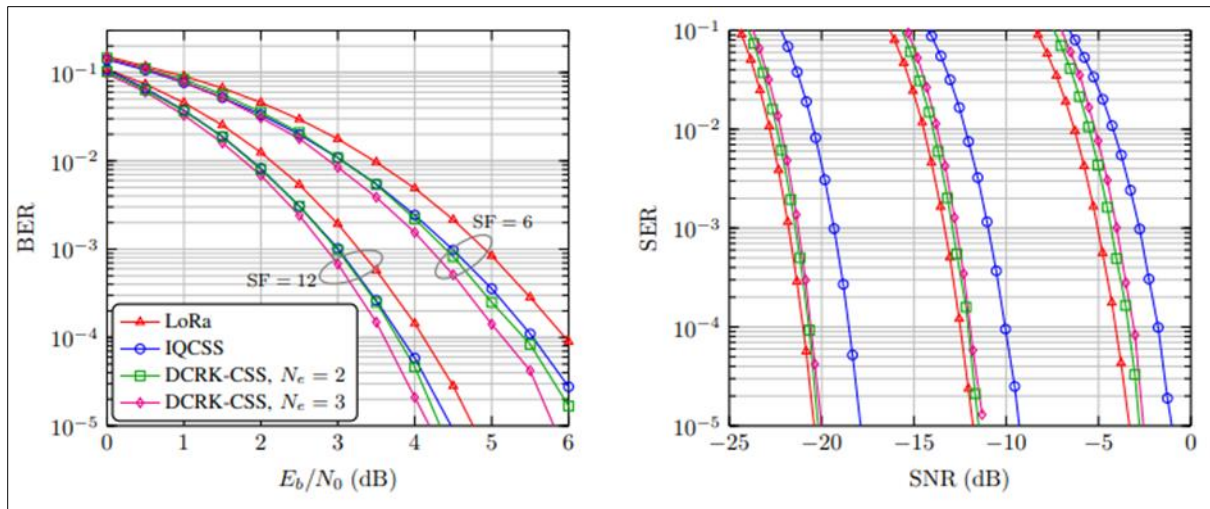
Table 3 Simulation parameter

Parameter	Value
Spreading factor	$SF \in \{6,9,12\}$
Extra information bits	$N_e \in \{2,3\}$
Bandwidth	250 kHz
Carrier frequency	863 MHz
Mobile speed	3 km/h
CP length	16 samples
TV channel	Single tap (Rayleigh)

6.3. Symbol and Bit Error Ratio Analysis

AWGN Channel: Figures 12 (a) and (b) show the estimated BER under AWGN channel for LoRa, IQCSS, and DCRK-CSS and the signal-to-noise ratio versus symbol error ratio respectively. Note that IQCSS transmits twice the amount of bits when compared with LoRa, and DCRK-CSS transmits N_e extra bits. Larger SFs will result in better performance since all schemes transmit data using frequency modulation, and adding more symbols to the constellation does not reduce the minimum symbol distance. There is a gap of about 0.5 dB between the curves of IQCSS and LoRa for the same SF, whereas between LoRa and DCRK-CSS the gap increases with E/N . The gap between LoRa and IQCSS is observed because collects less noise than LoRa in the process of detection, since it explores the phase information instead of making a decision based solely on the estimated energy of the frequency bins. Thus, one can use less energy to transmit more information with the same bit error probability when employing IQCSS over LoRa. However, the gap between LoRa and DCRK-CSS is observed due to the smaller average energy bit required to maintain an equal BER, and this gap

increases as the number of extra bits encoded on the chirp slope increases. Nevertheless, note that for the lower E_b/N_0 regime, the gap is reduced when compared with the high E_b/N_0 regime, this is observed since the different despreading signals are not completely orthogonal to each other, but rather present a significant low correlation.



(a) Average bit energy versus bit error ratio. (b) Signal-to-noise ratio versus symbol error ratio.

Figure 12 Error performance under AWGN channel

7. Conclusion

LoRaWAN is becoming one of the key protocols for IoT enablers for the future, enabling cost and energy efficient communication solutions for myriads of low-end transducers. Smart home automation, smart healthcare and wellbeing monitoring, and environment monitoring are just a few potential fields where these technologies can find wide utilization. In most of these applications the data need to be delivered to the IoT cloud, where they are collectively stored and made available to the interested parties using proper interfaces and authentication mechanisms. One of the efficient mechanisms to support this is to use the 3GPP cellular network interfaces and infrastructure already deployed, which calls for integration of the LoRaWAN and the cellular systems.

In this paper, we have reviewed the LoRa protocol stack and the benefit of adopting it for IoT. In addition to that, this paper has presented the various possible ways of integrating LoRaWAN and 5G for effective communication in high-bandwidth requirements.

Compliance with ethical standards

Acknowledgments

The authors are grateful to Dr Denis Mwigusa of Nelson Mandela Institute of Science and Technology in Tanzania for his guidance in accomplishing this work. The authors also thank Dr Asinta Manyele and Dr Mbazigwa Mkiramweni both of DIT for his encouragement toward research and publications.

Disclosure of conflict of interest

The authors declare that no conflict of interest exists.

References

- [1] LoRa Alliance. <https://lora-alliance.org/>
- [2] <https://www.rfwireless-world.com/Terminology/Advantages-and-Disadvantages-of-Lora-or-LoRaWAN.html>

- [3] J. Sanchez-Gomez, R. Sanchez-Iborra, and A. Skarmeta, "Transmission technologies comparison for IoT communications in smart-cities," in GLOBECOM 2017 - 2017 IEEE Global Communications Conference, pp. 1–6, Dec 2017
- [4] F. Adelantado, X. Vilajosana, P. Tuset-Peiro, B. Martinez, J. MeliaSegui, and T. Watteyne, "Understanding the limits of LoRaWAN," IEEE Communications Magazine, vol. 55, pp. 34–40, Sep. 2017.
- [5] M. Hanif and H. H. Nguyen, "Slope-shift keying lora-based modulation," IEEE Internet of Things Journal, vol. 8, no. 1, pp. 211–221, 2021
- [6] [https://www.iotone.com/iotone100/IoT companies](https://www.iotone.com/iotone100/IoT%20companies)
- [7] M. Hanif and H. H. Nguyen, "Slope-shift keying lora-based modulation," IEEE Internet of Things Journal, vol. 8, no. 1, pp. 211–221, 2021.
- [8] A. Knapp and L. Pap, "Performance analysis of pulse position based chirp spread spectrum technique for multiple access," in 2017 25th International Conference on Software, Telecommunications and Computer Networks (SoftCOM), pp. 1–5, 2017.
- [9] A. Mahmood, E. Sisinni, L. Guntupalli, R. Rondon, S. A. Hassan, and M. Gidlund, "Scalability analysis of a lora network under imperfect orthogonality," IEEE Transactions on Industrial Informatics, vol. 15, no. 3, pp. 1425–1436, 2019.
- [10] D. Croce, M. Gucciardo, S. Mangione, G. Santaromita, and I. Tinnirello, "Impact of LoRa imperfect orthogonality: Analysis of link-level performance," IEEE Communications Letters, vol. 22, pp. 796–799, April 2018.
- [11] M. El-Aasser, A. Gasser, M. Ashour, and T. Elshabrawy, "Performance analysis comparison between lora and frequency hopping-based lpwan," in 2019 IEEE Global Conference on Internet of Things (GCIoT), pp. 1–6, 2019.
- [12] I. Bizon Franco de Almeida, M. Chafii, A. Nimr, and G. P. Fettweis, "Inphase and quadrature chirp spread spectrum for IoT communications," in 2020 IEEE Global Communications Conference: Selected Areas in Communications: Internet of Things and Smart Connected Communities (Globecom2020 SAC IoTSCC), (Taipei, Taiwan), Dec. 2020.
- [13] Semtech Corporation, SX1272/73 - 860 MHz to 1020 MHz Low Power Long Range Transceiver Datasheet, January, 2019.
- [14] "The thing Network", <https://www.thethingsnetwork.org/docs>
- [15] A. J. Wixted, P. Kinnaird, H. Larijani, A. Tait, A. Ahmadinia and N. Strachan, "Evaluation of LoRa and LoRaWAN for wireless sensor networks," 2016 IEEE SENSORS, 2016, pp. 1-3, doi: 10.1109/ICSENS.2016.7808712.
- [16] L. Vangelista, "Frequency shift chirp modulation: The lora modulation," IEEE Signal Processing Letters, vol. 24, pp. 1818–1821, Dec 2017.
- [17] J. P. Bardyn et al., "IoT: The era of LPWAN is starting now", in ESSCIRC Conf. 2016, pp. 25-30.
- [18] M. Taneja, "LTE-LPWA networks for IoT applications", in ICTC, Jeju, 2016, pp. 396-399.
- [19] LoRaSim, <http://www.lancaster.ac.uk/scc/sites/lora/lorasim.html>. [22] M. C. Bor, U. Roedig, T. Voigt, and J. M. Alonso, "Do LoRa Low-Power Wide-Area Networks Scale?" in Proceedings of the 19th ACM International Conference on Modeling, Analysis and Simulation of Wireless and Mobile Systems, pp. 59–67, Malta, Malta, 2016.
- [20] Point-to-Point Protocol, <https://www.juniper.net/>.
- [21] L. Vangelista, "Frequency shift chirp modulation: The lora modulation," IEEE Signal Processing Letters, vol. 24, pp. 1818–1821, Dec 2017.
- [22] Kamanga, Isaack & Lyimo, Johanson. (2022). Mobile Network Access Points using Self Organising Drone Constellations. International Journal of Computer (IJC). 45. 81-94. URL: <https://ijcjournal.org/index.php/InternationalJournalOfComputer/article/view/1980/729>